Development of Anthropometric Specifications for the Large-Male Warrior Injury Assessment Manikin (WIAMan)

Matthew P. Reed

Biosciences Group
University of Michigan Transportation Research Institute

May 2022

UNCLASSIFIED: Distribution Statement A. Approved for public release. OPSEC#6403

Development of Anthropometric Specifications for the Large-Male Warrior Injury Assessment Manikin (WIAMan)

Final Report

UMTRI-2022-7

by

Matthew P. Reed

University of Michigan Transportation Research Institute

May 2022

REPORT DOCUMENTATION PAGE

Form Approved
OMB No. 0704-0188

Public reporting burden for this collection of information is estimated to average 1 hour per response, including the time for reviewing instructions, searching existing data sources, gathering and maintaining the data needed, and completing and reviewing this collection of information. Send comments regarding this burden estimate or any other aspect of this collection of information, including suggestions for reducing this burden to Department of Defense, Washington Headquarters Services, Directorate for Information Operations and Reports (0704-0188), 1215 Jefferson Davis Highway, Suite 1204, Arlington, VA 22202-4302. Respondents should be aware that notwithstanding any other provision of law, no person shall be subject to any penalty for failing to comply with a collection of information if it does not display a currently valid OMB control number. **PLEASE DO NOT RETURN YOUR FORM TO THE ABOVE ADDRESS.**

1. REPORT DATE *(DD-MM-YYYY)*	2. REPORT TYPE	3. DATES COVERED *(From - To)*
May 31, 2022	Final Report	July 2021- May 2022

4. TITLE AND SUBTITLE

Development of Anthropometric Specifications for the Large-Male Warrior Injury Assessment Manikin (WIAMan)

5a. CONTRACT NUMBER

5b. GRANT NUMBER

5c. PROGRAM ELEMENT NUMBER

6. AUTHOR(S)

Reed, Matthew P.

5d. PROJECT NUMBER

5e. TASK NUMBER

5f. WORK UNIT NUMBER

7. PERFORMING ORGANIZATION NAME(S) AND ADDRESS(ES)

University of Michigan
Transportation Research Institute

8. PERFORMING ORGANIZATION REPORT

UMTRI-2022-7

9. SPONSORING / MONITORING AGENCY NAME(S) AND ADDRESS(ES)

US Army Ground Vehicle Systems Center

Warren, MI 48397-5000

10. SPONSOR/MONITOR'S ACRONYM(S)

11. SPONSOR/MONITOR'S REPORT NUMBER(S)

Issued Upon Submission

12. DISTRIBUTION / AVAILABILITY STATEMENT

13. SUPPLEMENTARY NOTES

14. ABSTRACT

Data from a previous study of soldier posture and body shape were analyzed to develop anthropometric specifications for an anthropomorphic test device (ATD) intended to represent a large-male Soldier for assessments of vehicle occupant protection in underbody blast. The large-male Warrior Injury Assessment Manikin (WIAMan) has target stature and body mass based on 95th-percentile values for male Soldiers in a recent Army study. Body landmarks and internal joint center locations were developed using data from 100 soldiers with a wide range of body size measured in a single squad seating condition. Regression methods were used to establish target values for the ATD. Laser scan data from 119 men in up to four seated postures were analyzed using principal component analysis and regression to obtain a statistical model predicting body shape as a function of overall body dimensions and surface landmark locations. Small adjustments to the posture and shape were made to obtain a symmetrical posture with the thighs horizontal and legs vertical. The head surface was generated through a statistical analysis of data from a separate study that included realistic scalp contours and face landmarks. Because the hand and foot shapes were not well measured in the whole-body scan data, scaled versions of the hand and foot were added. Pelvis geometry was generated through a statistical model based on data from medical images. The final anthropometric specification included the surface geometry as a polygonal model, internal joint centers and surface landmarks, and a polygonal model of the bony pelvis and sacrum.

15. SUBJECT TERMS

Anthropometry, Posture, Vehicle Occupants, Statistical Shape Analysis, Safety

16. SECURITY CLASSIFICATION OF:			17. LIMITATION OF ABSTRACT	18. NUMBER OF PAGES	19a. NAME OF RESPONSIBLE PERSON M.P. Reed
a. REPORT UNCLASSIFIED, Dist A.	b. ABSTRACT UNCLASSIFIED, Dist A.	c. THIS PAGE UNCLASSIFIED, Dist A.		34	19b. TELEPHONE NUMBER *(include area code)* (734) 936-1111

Standard Form 298 (Rev. 8-98)
Prescribed by ANSI Std. Z39.18

ACKNOWLEDGMENTS

This work was supported by the U.S. Army Ground Vehicle Systems Center. The data used for the current analysis were gathered in a 2012 study. I would like to thank the over 300 Soldiers who participated in the Seated Soldier Study, providing data that are improving safety and accommodation for the next generation of soldiers. I am grateful to Sheila Ebert, who led the initial data processing and analysis of this dataset and supported the current analysis. Thanks to Steve Moss and the rest of the team at Diversified Technical Systems who provided valuable feedback as they developed the large-male WIAMan design based in part on the results of this project.

CONTENTS

ABSTRACT

Data from a previous study of soldier posture and body shape were analyzed to develop anthropometric specifications for an anthropomorphic test device (ATD) intended to represent a large-male Soldier for assessments of vehicle occupant protection in underbody blast. The large-male Warrior Injury Assessment Manikin (WIAMan) has target stature and body mass based on 95th-percentile values for male Soldiers in a recent Army study. Body landmarks and internal joint center locations were developed using data from 100 soldiers with a wide range of body size measured in a single squad seating condition. Regression methods were used to establish target values for the ATD. Laser scan data from 119 men in up to four seated postures were analyzed using principal component analysis and regression to obtain a statistical model predicting body shape as a function of overall body dimensions and surface landmark locations. Small adjustments to the posture and shape were made to obtain a symmetrical posture with the thighs horizontal and legs vertical. The head surface was generated through a statistical analysis of data from a separate study that included realistic scalp contours and face landmarks. Because the hand and foot shapes were not well measured in the whole-body scan data, scaled versions of the hand and foot were added. Pelvis geometry was generated through a statistical model based on data from medical images. The final anthropometric specification included the surface geometry as a polygonal model, internal joint centers and surface landmarks, and a polygonal model of the bony pelvis and sacrum.

INTRODUCTION

The Warrior Injury Assessment Manikin (WIAMan) program developed a midsize-male anthropomorphic test device (ATD) for use in underbody blast testing of military vehicles and vehicle components. The anthropometric specifications for the ATD, including the body size, shape, and design posture, were developed based on detailed anthropometric data from Soldiers (Reed 2013). The reference body dimensions for the midsize-male WIAMan were based on 50th-percentile values for stature and body weight from a pilot study (Paquette et al. 2009) for the 2012 U.S. Army anthropometry survey, known as ANSUR II (Gordon et al. 2014). The midsize-male WIAMan was the first ATD to be based on a statistical analysis of 3D body shape data.

This report presents the development of anthropometric specifications for a large-male WIAMan ATD. The reference values for stature and body weight correspond to 95th-percentile values from ANSUR II. The data were drawn from the Seated Soldier Study (Reed and Ebert 2013), the same data source for the midsize male. The analysis methods were similar, but new data sources were used for the head and pelvis, and a new symmetrical template was used for the body shape analysis.

Table 1 lists the four components of the analysis. The posture target, which consists of surface landmark and internal joint center locations, was developed based on a regression analysis of landmark data from 100 male Soldiers measured in a seat with a horizontal seat pan and vertical seat back. A statistical body shape model was created by analyzing 300 3D laser scans from 119 men who were each measured in up to four seated postures with varying levels of recline. A regression model was created to predict the body shape from overall body dimensions and a subset of the landmarks predicted for the target posture. Additional internal joint centers were interpolated to better define the spine posture. Generic hand and foot shapes were added to address limitations in the scan-based statistical model, and the posture was adjusted to the desired design posture with thighs horizontal and upper extremities in a relaxed posture.

A new 3D head shape model with an accurate scalp was available from recent work (Park et al. 2021). The male data from that study were re-analyzed to obtain an appropriate head shape, which was aligned with the whole-body shape model using surface landmarks. A larger and more-detailed set of bone shape data were also available (Brynskog et al. 2021). A regression analysis based on bispinous breadth was used to obtain the target pelvis bone landmark configuration. These landmark data were mapped to a new 3D pelvis surface model to generate the target for the ATD.

The final body representation was compared quantitively and qualitatively with other large-male representations based on similar overall body dimensions. The Anthropometry of Motor Vehicle Occupants (AMVO) study from the 1980s developed specifications for a large-male ATD with a reference stature similar to the current work (Schneider et al. 1983). The current results were also compared with a body shape generated from a statistical model of civilian adults (Park et al. 2021a).

Table 1
Summary of Analyses, Methods, and Outcomes

Analysis	Data Source	Analysis Method	Outcome
1. Posture analysis for the WIAMan anthropometry target	Body landmark locations measured in Seated Soldier Study, squad condition C01 (N=100)	Regression using target stature, body weight, and ratio of sitting height to stature	Tabular data on landmark and joint locations
2. External body shape	Whole-body laser scan data in minimally clad condition, up to four seated postures per participant (N=300 scans from 119 Soldiers)	Surface template fitting followed by principal component and regression analyses	Body surface described by a polygonal mesh with 14454 polygons corresponding to the target body dimensions and landmark locations from Analysis 1
3. Pelvis geometry	CT image analysis (N=132)	Regression analysis of landmark locations	Target landmarks and polygonal surface mesh in position
4. Head geometry	Male head surface data with complete scalp and manually identified landmarks (N=80)	Regression on combined landmark and mesh vertices	Target head shape with surface landmarks in position

METHODS

Reference Body Dimensions

The large-male WIAMan is intended to represent a "95th-percentile" Soldier. However, the target specification is better stated as "the average body size and shape for a U.S. male Soldier who is 95th percentile by stature and body weight." Because the design posture for the ATD is seated, only the target body weight can be specified directly for the design from standard anthropometric data. All other dimensions must be obtained through analysis of data from subjects who vary relative to the target values.

The reference database is ANSUR II (Gordon et al. 2012). Table 2 shows the target values for stature and body weight along with comparative values from other sources. Note that although the distribution of male stature for both military and civilian populations in the US has remained approximately the same for the past 40 years, body weight has trended upward, particularly in the upper tails of the distribution. Hence, the target body weight of 110.7 kg (244 lb) is markedly higher than the civilian value from the 1980s used in the specification of the Hybrid-III "95th-percentile" male. The stature value from the US Army 1988 ANSUR survey is similar to the current value, but the current body weight value is 10 kg (22 lb) higher than the corresponding value from 1988. For reference, the current 95th-percentile values for U.S. civilian men ages 20-29 (Fryar et al. 2021) are similar for stature but much higher for body weight.

Table 2
Male Reference Dimensions Compared with Previous Studies

Dimension (95th-percentile values)	WIAMan Target*	ANSUR 88**	Large-Male AMVO Target (Schneider et al. 1983)	Hybrid-III (95th-percentile)†	Civilians Ages 20-29††
Stature (mm)	1870	1868	1869	1880	1871
Body Mass (kg)	110.7	100.6	102.3	102	128
BMI*** (kg/m^2)	31.7	28.9	29.3	28.9	36.6
Stature (in)	73.6	73.5	73.6	74.0	73.7
Body Mass (lb)	244	222	226	225	282

* ANSUR II
** 95th-percentile male values
*** BMI for the 95th-percentile values of stature and weight, rather than 95th-percentile BMI.
† Reference values from Mertz et al. 2001
†† Values for civilian men ages 20-29 years from Fryar et al. 2021.

Posture Analysis

Data from 100 men measured in the Seated Soldier Study (Reed and Ebert 2013) were used for the posture analysis. Stature ranged from 1602 to 1965 mm (mean 1759 mm) and body mass index from 18.2 to 38.3 kg/m^2 (mean 26.7 kg/m^2).

Soldiers were instructed to sit comfortably in the seat shown in Figure 1. Lower and upper extremity postures were required to be approximately symmetrical. A FARO Arm coordinate digitizer was used to record body landmark locations defining the seated posture. The posture data for the current analysis were extracted from Condition C01, in which the padded seat back was nominally vertical, the padded seat cushion was nominally horizontal, and the seat height above the floor (measured from SAE J826 H-point) was 450 mm (for more details, see Reed and Ebert 2013). The current analysis was conducted using data from conditions in which soldiers wore their Advanced Combat Uniform (ACU), including boots. No other protective equipment or gear was worn. The soldier donned a five-point harness in each condition after selecting a comfortable posture. Figure 1 shows a soldier in condition C01 with the ACU garb level.

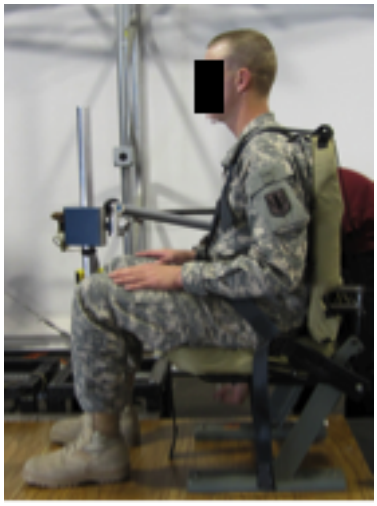

Figure 1. Soldier in Condition C01 and the ACU garb level.

Hardseat Data and Analysis

Additional data obtained in a laboratory hardseat, shown in Figure 2, were used to augment the data from the padded test seat. The hardseat provided access to posterior landmarks, enabling a more accurate characterization of each soldier's pelvis and spine geometry. These data were used to estimate pelvis and spine joint center locations relative to surface landmarks. The relationships between the anterior landmarks accessible in the squad seat and the joints were used to estimate joint center locations in the squad seating conditions. For more details on these calculation procedures, see Reed and Ebert (2013).

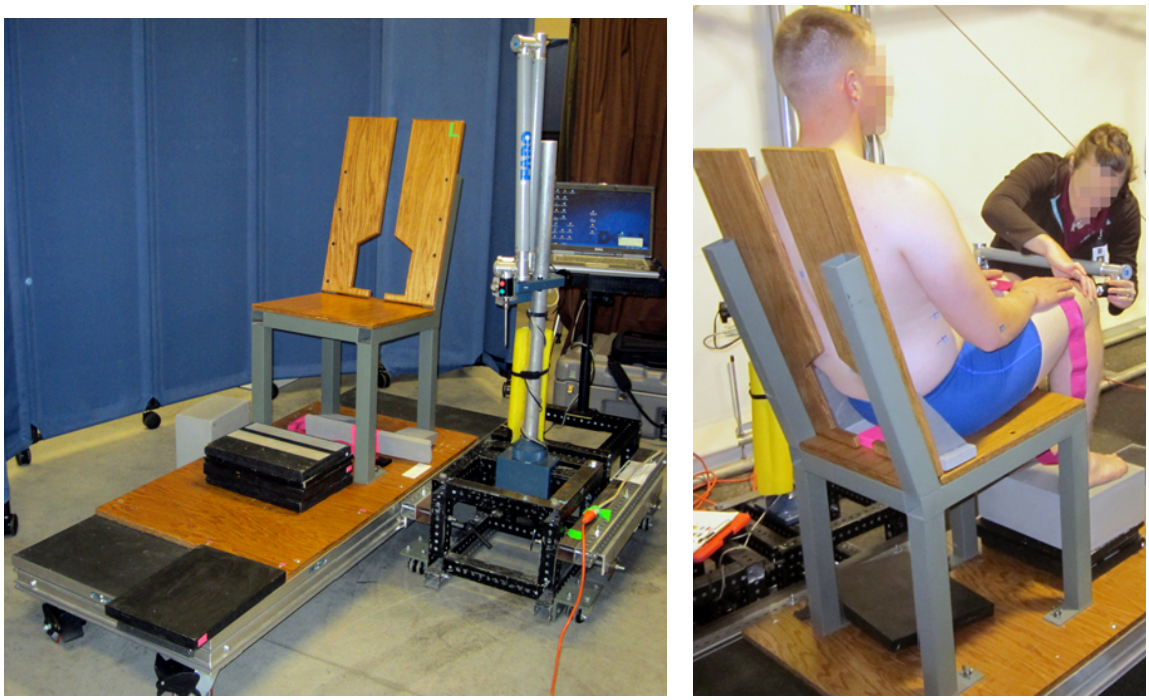

Figure 2. Laboratory hardseat used to obtain additional skeletal geometry information. Note the blue dots on the skin that mark landmarks to be digitized. A nylon strap was used to control leg splay, maintaining the femurs approximately parallel.

Body Landmark and Joint Analysis Methodology

The goal of the landmark analysis was to obtain a consistent set of landmarks and joint center location estimates for individuals who match the reference body dimensions. In most previous analyses of this type (e.g., AMVO), data from individuals judged to be "close" to the reference size were averaged. The current analysis uses a more rigorous regression procedure that allows data from individuals with a wide range of body size to be used. Each landmark or joint coordinate is regressed on stature, body mass index, and the ratio of sitting height to stature. The reference values described above are then input to the resulting equations. To facilitate the interpretation of the analysis, the regressions were performed on principal components (PCs) of the covariance matrix of the landmark coordinates, but all PCs were retained, so the results are equivalent to regression on the individual coordinates. No tests of statistical significance were performed, because excluding non-significant terms would result in inconsistencies across landmarks in trends with body size. For example, BMI was included as a predictor in the regression models for all PCs, even though it was only statistically significant for a few of the PCs.

A rationalization process was applied to obtain symmetrical landmarks. The Y (lateral) coordinates of landmarks on the midline of the body were assigned a value of zero, eliminating small asymmetries, typically less than a millimeter, that remained after the statistical modeling process. Bilateral pairs of landmarks (for example, left and right acromion) were assigned X and Z values equal to the means of the respective points, and the Y values were set to ± 50% of the initial Y-axis difference between the points.

The output of this analysis and rationalization process was a list of landmark and joint locations that represent the initial target for the ATD. As noted below, some additional posture adjustments were conducted to obtain the desired reference posture.

External Body Shape

Laser Scan Data Processing

Laser scan data obtained from minimally clad soldiers were obtained in the Seated Soldier Study. A total of 300 scans from 119 male soldiers were used, with up to four scan postures per soldier (not all soldiers were scanned in all conditions). Figure 3 shows the postures. Due to the study design, this is a different subset of the participants than was used for the posture analysis. Note that the analysis techniques are robust to differences in the samples. Surface body landmark locations were extracted from the scan data, as described in Reed and Ebert (2013).

The current analysis used a template mesh that differed from the one used in Reed (2013) for the midsize male. The new template is symmetrical and based on quadrilaterals rather than triangles. Figure 4 shows the template, example data with landmarks, the template initially morphed to match the data at a subset of the landmarks, and the result after final template fitting. A second round of template fitting was conducted using a "bootstrap" prediction model. That is, a statistical body shape model was generated using the data from the first round of fitting that predicted body shape from the landmarks. This was used in place of the landmark-based morphing step for the second round of fitting.

To generate the final statistical body shape model, a principal component analysis (PCA) was conducted on the vertex coordinates. For the subsequent regression analysis to predict body shape, 60 of 126 PCs representing over 99 percent of the variance in the coordinate data were retained.

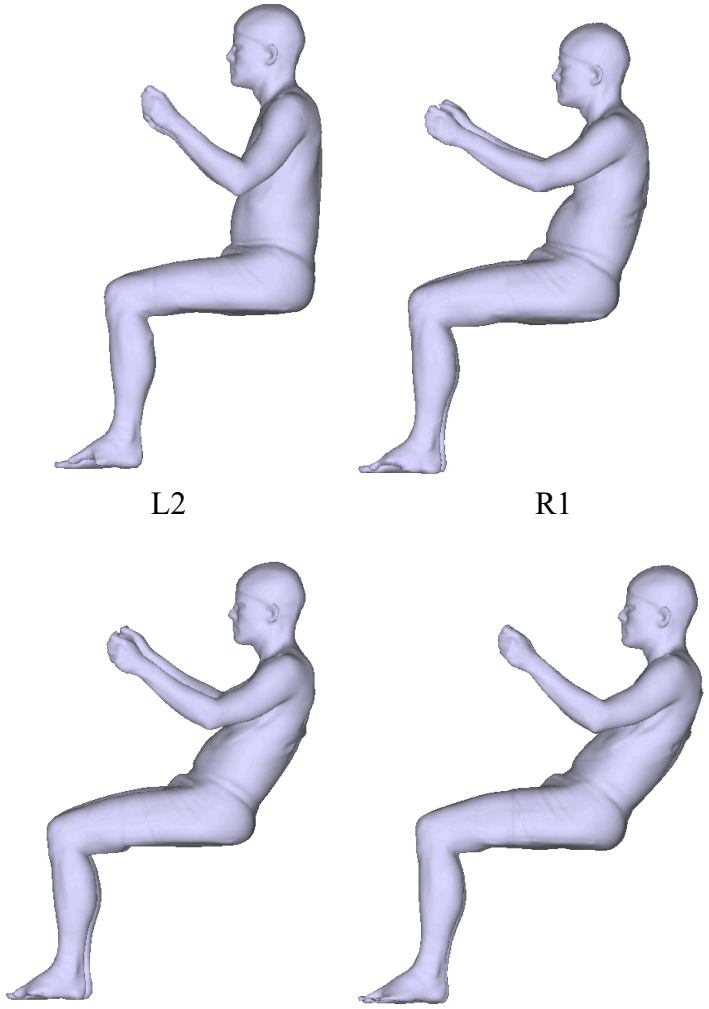

Figure 3. The four scan postures used for the current analysis. Postures R1, R2, and R3 were supported by a small, padded backrest (see Reed and Ebert 2013 for details).

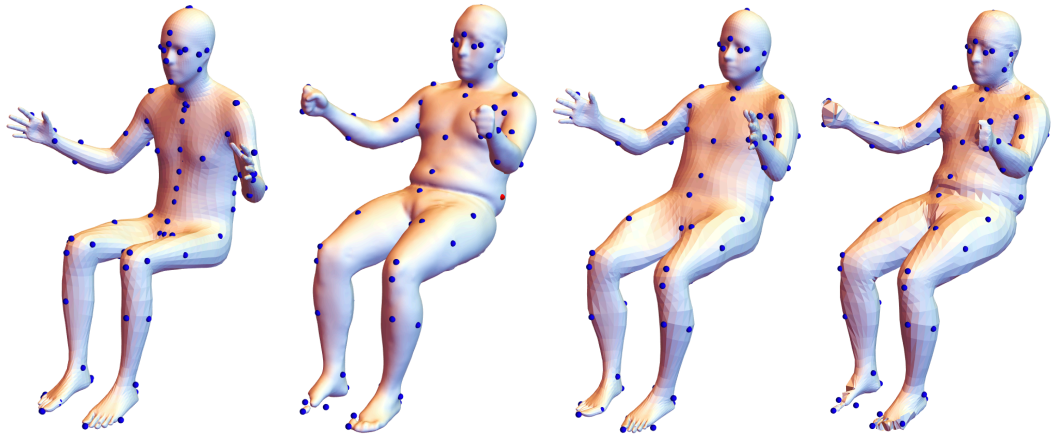

A B C D

Figure 4. Template with landmarks (A), sample scan with landmarks (B), the template morphed to match the data at individual landmarks (C), and the result of final template fitting to the scan (D).

The body shape analysis proceeded somewhat differently from the landmark analysis. One approach would be to conduct a regression analysis to predict PC scores from the reference body dimensions in the same manner as with the landmark data. However, because the scan and landmark data were drawn from different subjects in different conditions, some discrepancies would inevitably emerge. Consequently, a set of landmark joint locations were used along with the body dimensions as input to the body shape predictions. Table 3 lists the landmarks and joints. All landmarks and joints were included in the PCA of the body shape data, enabling verification that the landmark and joint targets were met (all discrepancies < 0.1 mm).

Table 3
Surface Landmarks and Joints Used Along with Stature, BMI, and the Ratio of Sitting Height to Stature To Predict Surface

Glabella_Ct_L	SpineT04_Ct_M
Tragion_Rt_L	SpineT12_Ct_M
Tragion_Lt_L	SpineL03_Ct_M
Suprasternale_Ct_L	L5S1Joint
Substernale_Ct_L	HipJntRt
SpineC07_Ct_M	HipJntLt

Posture Adjustment

The desired design posture for the WIAMan included a horizontal thigh segment, a vertical leg, and a relaxed upper-extremity posture. Because the posture and body shape data were obtained with a different seat height and arm posture, the posture of the predicted body shape was adjusted using linear blend skinning. Under this common approach to pose modification, each vertex in the model is assigned a weight for each adjacent body segment. For example, joints near the elbow have weights for the forearm and arm segments. When the model is articulated, each vertex is moved according to the weights for these segments. The result is a smooth blending at the joints.

Spine Joint Interpolation

The surface landmark data were used directly to estimate spine joints at the atlanto-occipital junction, C7/T1, T12/L1, and L5/S1. To provide additional guidance for ATD design, the intervening joint centers, defined as the estimated geometric centers of the intervertebral disks, were estimated from the surface contour by interpolating between the previously calculated joint centers. The motion segment heights (e.g., L4/L5 to L5/S1) were determined as fractions of the lumbar, thoracic, and cervical chord lengths using data from Black et al. (1991).

Head Geometry

The whole-body surface model uses data from a laser scanner that does not provide a high level of detail on the face and head. Moreover, the data are affected by hair artifacts, such that the scalp shape is not accurately captured. For the midsize male WIAMan, an analysis of head and face landmark and measurement data was used to morph a reference head model (Reed and Corner 2013). However, a new model based on detailed head scans from 80 bald men was available for the large-male analysis (Park et al. 2021b). A statistical model created from these data was generated using the same template mesh used for the whole-body modeling. A total of 58 manually identified landmarks were included in the statistical model, which predicted head shape from head length, head breadth, and tragion to top of head. These manually measured dimensiolens are available in the ANSUR II dataset. A regression analysis using ANSUR II using stature and BMI as predictors gave target values of length = 206 mm, breadth = 157 mm, and tragion to top of head = 134 mm (Table 4). These values were used to generate a head model that was then slightly scaled (less than 3 mm per axis) to match the target values. Table 4 demonstrates that because the head dimensions are not highly correlated with stature or body weight, the percentage increase in head dimensions between the midsize male and large male is smaller than the increase in overall body dimensions.

Table 4
Comparison of Midsize-Male and Large-Male Target Head Dimensions†

	Stature (mm)	Weight (kg)	BMI (kg/m^2)	Head Length (mm)	Head Breadth (mm)	Tragion to Top of Head (mm)
Midsize Male	1755	84.2	27.3	199	154	131
Large Male	1870	110.7	31.7	206	157	134
Ratio*	6.6%	31.5%	16.1%	3.5%	1.9%	2.3%

* (large male – midsize male)/midsize male * 100%
† Note that ATD head may have different dimensions due to design, manufacturing, and performance requirements.

Pelvis Geometry

The external body landmark measurements obtained in the Seated Soldier study provided good information on the position and orientation of the pelvis, but the data are insufficient to specify the overall size and shape of the pelvis. To provide detailed guidance for ATD design, an analysis of medical imaging data was conducted.

The current analysis used a larger dataset than was used for the midsize male. Brynskog et al. (2021) extracted 286 landmarks from each of 57 male and 74 female pelves extracted from computed tomography (CT) studies of adults with a wide range of body size. For the current analysis, a regression model expressed the landmark locations as a function of bispinous breadth (distance between the anterior-superior iliac spine landmarks). The regression model included an interaction term for sex. The target bispinous breadth was obtained by regression in the ANSUR dataset (Gordon et al. 1989), which includes manually measured bispinous breadth (bispinous breadth is not available in ANSUR II). The target value for 1870 mm stature was given by 66.9 + 0.0938*stature = 242 mm. Note that because pelvis size is only weakly correlated with overall body size, the target value is only 11 mm larger than the target value for the midsize male.

The predicted landmarks were rationalized by making the left and right sides symmetrical and assigning landmarks on the mid-sagittal plane a lateral coordinate value of zero. The resulting landmark configuration was then translated and rotated to align with joint locations estimated from the surface body landmarks. A generic midsize-male pelvis surface model developed in previous UMTRI research was morphed to the current target using radial-basis-function techniques (Bennink et al. 2007) to match the target landmark configuration, providing geometric guidance for the overall bony pelvis and sacrum.

Hands and Feet

During the development of the midsize-male WIAMan ATD, a substantial amount of design effort was needed to adapt the target foot model from Reed and Corner (2013) to the ATD, which requires a contoured sole to fit appropriately in a boot. The hand, which has minimal importance for the performance of this ATD, was created by scaling existing geometry.

Consequently, for the large-male ATD, scale factors were generated that could be used to adjust the midsize-male WIAMan hand and foot geometry to the large-male targets. The scale factors were generated using ANSUR II male data by the following process:

1. Select reference dimensions: foot length, foot breadth, ankle height, hand length, and hand breadth.
2. Generate linear regression equations predicting the dimensions from stature and BMI.
3. Using the regression equations, compute expected values for the midsize male and large male.

4. Calculate the expansion ratios as a percentage: (large male value – midsize mal)/(midsize male value) * 100%

For the foot, the scale factors were +7%, +6%, and +8% for the length, width, and height, respectively. For the hand, +6% for both length and width. Note that these are very close to the ratio based on stature (1870-1755)/1755 = +6.6%.

RESULTS

Posture Analysis for the WIAMan Anthropometry Target

Landmarks and Joints

Tables 5A-5C list landmark and joint locations calculated using the regression methods described above. The X axis is positive rearward, the Y axis is positive to the right, and the Z axis is positive upward. The origin is the midpoint between the hip joint centers. The thigh segments (hip to knee) are in the horizontal plane through the hips, and the ankles are in the vertical sagittal plane through the knee joints.

Table 5A
Extremity Joint Centers (mm)

Name*	X (fore-aft)	Y (lateral)	Z (vertical
ShoulderJnt_L	31.3	-202.8	467.5
ElbowJnt_L	-48.1	-264.6	165.9
WristJnt_L	-335.6	-198.8	162.6
KneeJnt_L	-482.1	-116.7	0
AnkleJnt_L	-482.1	-116.7	-457.3
HipJnt_R	0	91	0
HipJnt_L	0	-91	0
ShoulderJnt_R	31.3	202.8	467.5
ElbowJnt_R	-48.1	264.6	165.9
WristJnt_R	-335.6	198.8	162.6
KneeJnt_R	-482.1	116.7	0
AnkleJnt_R	-482.1	116.7	-457.3

Table 5B
Surface Landmarks (mm)

Name*	X (fore-aft)	Y (lateral)	Z (vertical
Suprasternale	-18	0	489.4
Substernale	-58.5	0	285.2
C7Surface	93.2	0	580.7
T4Surface	160.9	0	487
T8Surface	203.8	0	368.3
T12Surface	204.7	0	234.6
L1Surface	201.2	0	193.5
L2Surface	195.4	0	160.1
L3Surface	188.9	0	129.2
L4Surface	181.6	0	101
L5Surface	172.6	0	72.3
Tragion_L	10.3	-80	686.7
Acromion_L	13.9	-201.1	519.9
HumeralEpiCon_Lat_L	-45.2	-303.1	174.7
Wrist_Lat_L	-342.4	-220.9	156.5
FemoralEpiCon_Lat_L	-461	-177.8	-2.4
Suprapatella_L	-507.9	-122	51.5
Infrapatella_L	-539.1	-122	-3.9
Malleolus_Lat_L	-469.2	-144.7	-450.5
Tragion_R	10.3	80	686.7
Acromion_Ant_R	13.9	201.1	519.9
HumeralEpiCon_Lat_R	-45.2	303.1	174.7
Wrist_Lat_R	-342.4	220.9	156.5
FemoralEpiCon_Lat_R	-461	177.8	-2.4
Suprapatella_R	-507.9	122	51.5
Infrapatella_R	-539.1	122	-3.9
Malleolus_Lat_R	-469.2	144.7	-450.5
ASIS_L	-6.9	-123.3	100.2
ASIS_R	-6.9	123.3	100.2

* Suffixes L and R indicate the left and right side of the body, respectively. Origin is midpoint between the hip joint centers.

Table 5C
Spine Joint Centers (mm)

Name*	X (fore-aft)	Y (lateral)	Z (vertical
L5S1Joint	86.1	0	71.1
L4L5Joint	94.7	0	108.8
L3L4Joint	102.7	0	146.6
L2L3Joint	109.1	0	184
L1L2Joint	113.5	0	220.7
T12L1Joint	118.1	0	256.3
T11T12Joint	122.9	0	288.6
T10T11Joint	126.2	0	318.7
T9T10Joint	127.2	0	347.3
T8T9Joint	125.6	0	374.2
T7T8Joint	121.2	0	399.8
T6T7Joint	114	0	424.4
T5T6Joint	104.8	0	447.6
T4T5Joint	93.9	0	469.5
T3T4Joint	82	0	489.9
T2T3Joint	69.2	0	509
T1T2Joint	56.1	0	526.5
C7T1Joint	42.9	0	542.6
C6C7Joint	49.3	0	545
C5C6Joint	39.3	0	560.2
C4C5Joint	32.4	0	575.5
C3C4Joint	26.9	0	591.3
C2C3Joint	23.1	0	608.1
C1C2Joint	21.3	0	625.8
HeadNeckJnt	21.7	0	662.8

* Spine joint centers are estimated at the geometric center of the associated disk. HeadNeckJnt (atlanto-occipital joint) is estimated at the geometric center of the arc of the occipital condyles.

Segment Length Comparison

One consideration in evaluating the current results is a comparison of the segment lengths with other "large male" representations (nominally "95th-percentile male"). Table 6 lists comparative data from AMVO, the "95th-percentile" Hybrid-III ATD, and SAE J826. Note that the AMVO values differ somewhat from the original publication in Schneider et al. (1983). To provide better comparability with the current work, the joint locations

were calculated using the methods in Reed et al. (1999) from the AMVO shell surface landmark locations.

The current values for neck, pelvis, arm, and forearm segments are within 6 mm of the AMVO values. The current thigh and leg segments are about 6% & 3% longer, respectively, than the AMVO values. This may be due in part to differences in the populations that were measured. Large differences are seen in the thorax and abdomen (lumbar) segments. The sum of the two segment lengths differs by only one mm, but the thorax in the current analysis is 31 mm shorter. This difference results from a major difference in the way the thorax length was estimated. Specifically, the current value is based on a statistical model of the thorax developed from analysis of CT data (Wang et al. 2016). We regard this estimate as being more accurate than the estimates developed during the AMVO program in the 1980s, which used scaling relationships developed using a small set of lateral radiographs of men taken in an earlier study. The current analysis based on CT data indicates that the thorax segment length is on average approximately 61% of the total of the thorax and lumbar segment lengths for both men and women regardless of overall body size.

Table 6
Segment Length Comparison (mm)

Segment	Definition	Current	AMVO†	Hybrid-III*
Neck	AO-C7/T1	122	123	
Thorax	C7/T1-T12/L1	296	327	
Abdomen	T12/L1-L5/S1	188	156	
Pelvis	L5/S1-mean hip joint center	112	109	
Thigh	Hip-Knee	483	457	426
Leg	Knee-Ankle	457	444	434
Arm	Glenohumeral-Elbow	318	316	
Forearm	Elbow-Wrist	295	288	

† Joint locations in AMVO were calculated from the large-male shell landmark locations reported in Schneider et al. (1983) using methods from Reed et al. (1999) for improved consistency with the current methods.
* Obtained from Madymo model of large-male Hybrid-III.

External Body Shape

Figure 5 shows the initial body shape and landmarks generated from the statistical shape model using the target landmarks and body dimensions. The upper and lower extremity postures reflect the scan postures, which included a slight downward angle of the thighs and the upper extremities abducted and flexed at the shoulder and elbow. At this stage of

the analysis, the surface and landmarks are not yet symmetrical, and the head, hands, and feet are not yet finalized.

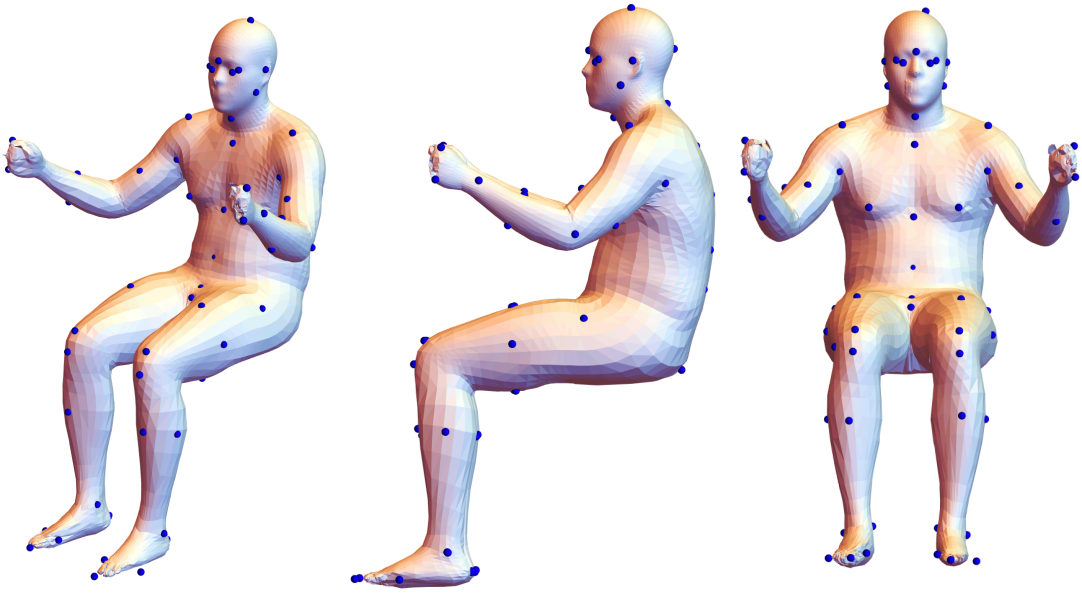

Figure 5. Body shape output from the regression model prior to posture and shape adjustments.

Figure 6 compares the predicted body shape after posture adjustment with the body shape target for the midsize-male WIAMan developed in prior work (Reed 2013). As expected, the torso and extremities are longer with greater depth, width, and circumference. The difference in head height above the hips is smaller than the seven percent difference in reference stature would suggest, and the difference in thigh length is greater, due to the lower extremities accounting for greater proportion of stature for taller men. Note that the treatment of the buttock and posterior thigh area was different for the current model. For the midsize-male model, the buttock and thigh areas were flattened to represent a flat, deformed contour. In contrast the large-male model contour is smoothed but not fully deformed, and the under-thigh artifacts caused by the scanning seat were not removed.

Figure 7 shows the target head geometry. The landmark locations in the whole-body coordinate system are listed in Tables 7A-7C. Because the head model was developed on the same mesh used for whole-body fitting, the head could be easily aligned and merged using the common landmarks. Figure 8 shows the head geometry overlaid with the midsize-male WIAMan target geometry.

Figure 8 shows the final body shape target with the internal joint centers and surface landmarks listed in Tables 5A-5C. The hands and feet are scaled from the original template and are not based directly on Soldier data. To provide a qualitative comparison of the body size and shape, the surface was overlaid with the AMVO large-male shell, aligning on the hip joint centers and rotating the more-reclined AMVO model to approximately align the torso (Figure 10). The overall body size is very similar. The WIAMan body shape has larger shoulders and thighs, and thinner abdomen, consistent with the younger, more-fit population represented by the Soldier manikin. Figure 111

shows a comparison with a body shape model based on civilian data (Park et al. 2021a). The inputs to the model were stature, BMI, and ratio of sitting height to stature (see HumanShape.org). As with the AVMO model, the Soldier body shape has thicker thighs and a thinner abdomen, but otherwise is similar in size.

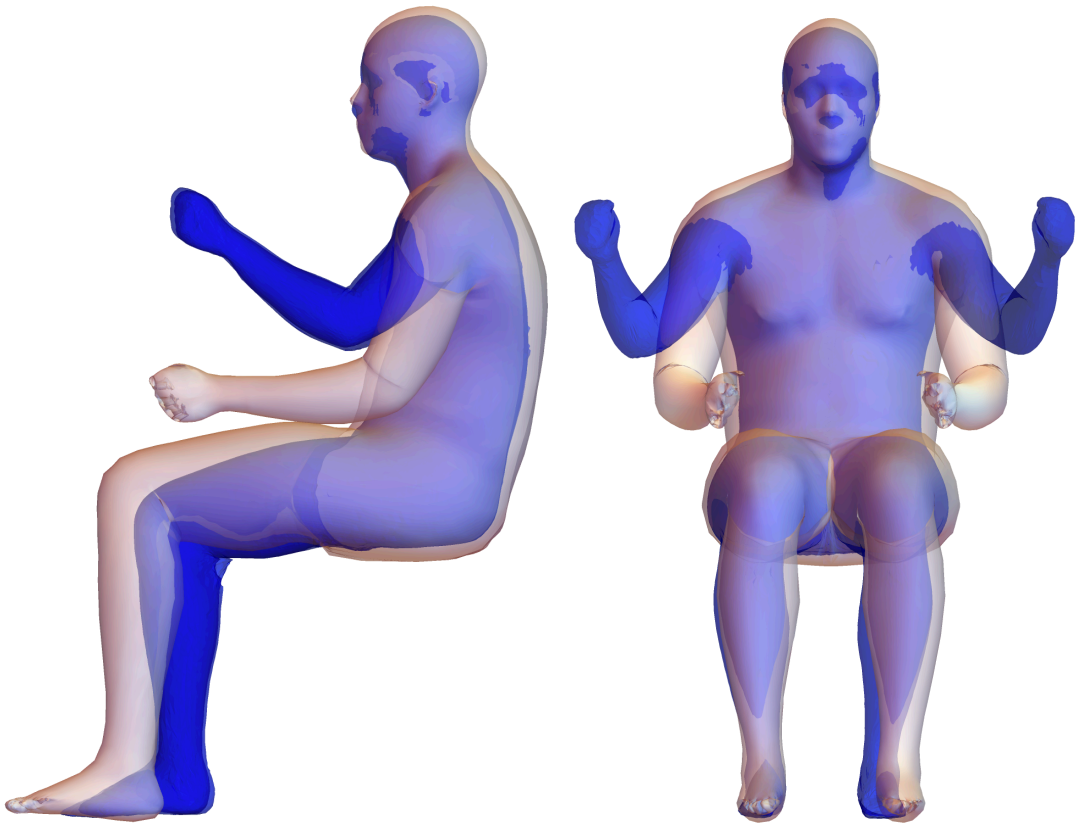

Figure 6. Comparison of midsize-male WIAMan external body shape target (blue) with large-male body shape. The large-male posture has been adjusted to design position.

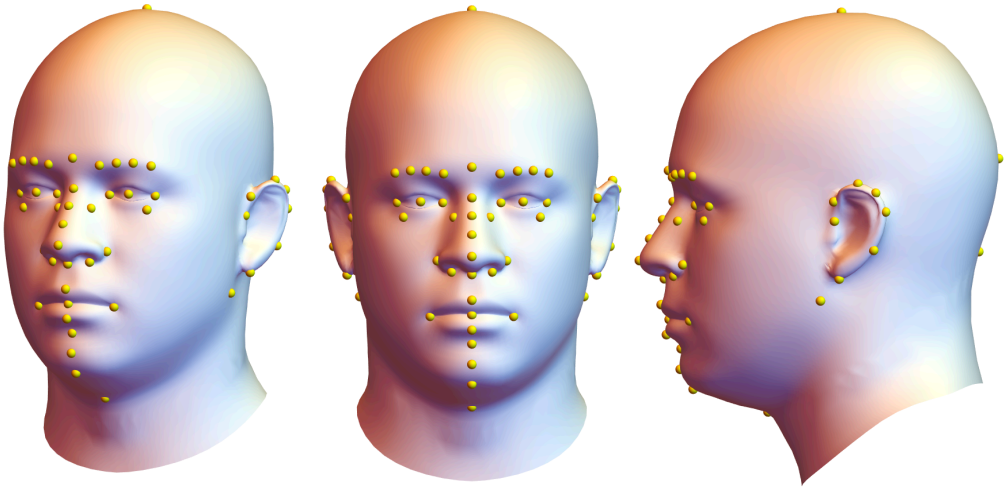

Figure 7. Head shape with landmarks.

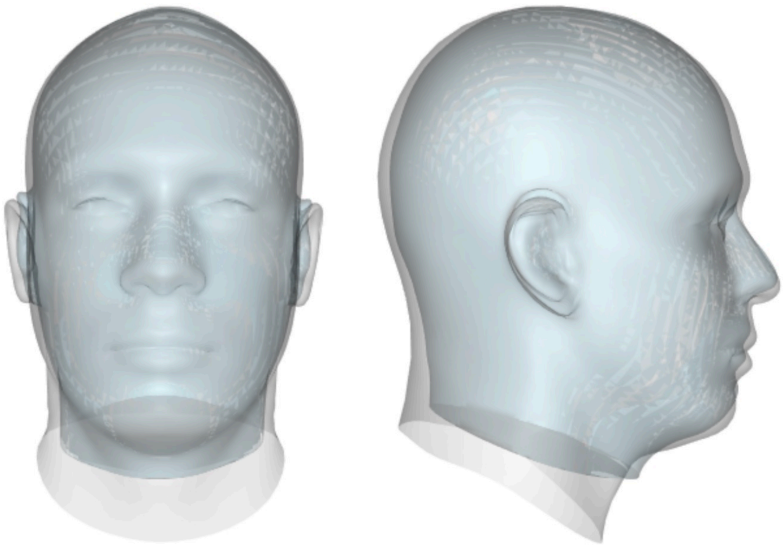

Figure 8. Overlay comparison of midsize-male (blue) and large-male target shapes (note that the ATD head shape is somewhat different due to design and manufacturing considerations).

Table 7A
Head Landmarks Group A (mm)

X	Y	Z	Landmark Name
10.3	-75.2	686.7	EarTragion_R
10.4	-78.9	698.9	Ear_Preaurale_R
25.9	-88.7	709.4	Ear_Superaurale_R
36.6	-91.2	703.3	Ear_Half_Super_Post_R
42.4	-90.2	691.3	Ear_Postaurale_R
34.1	-87	667.6	Ear_Half_Post_Sub_R
12	-78.6	650.4	Ear_Subaurale_R
10.3	75.2	686.7	EarTragion_L
10.4	78.9	698.9	Ear_Preaurale_L
25.9	88.7	709.4	Ear_Superaurale_L
36.6	91.2	703.3	Ear_Half_Super_Post_L
42.4	90.2	691.3	Ear_Postaurale_L
34.1	87	667.6	Ear_Half_Post_Sub_L
12	78.6	650.4	Ear_Subaurale_L
-75.9	-32.3	699.8	EyeCen_R
-75.9	32.3	699.8	EyeCen_L
-74	-18.2	699.1	Eye_CorMed_R
-74	18.2	699.1	Eye_CorMed_L
-67.1	-46.9	699	Eye_CorLat_R
-67.1	46.9	699	Eye_CorLat_L
-70.8	-32.5	686.7	Eye_Infraorbiatale_R
-70.8	32.5	686.7	Eye_Infraorbiatale_L
-75.2	0	688.7	Eye_CtInfraorbiatale_R
-75.2	0	688.7	Eye_CtInfraorbiatale_L

Table 7B
Head Landmarks Group B (mm)

X	Y	Z	Landmark Name
-89.6	-17.8	717.9	EyebrowMed_R
-87.7	-28.8	719.6	EyebrowMedQuart_R
-83.4	-38.6	719.7	EyebrowLatQuart_R
-77.1	-48.3	718	EyebrowLat_R
-89.6	17.8	717.9	EyebrowMed_L
-87.7	28.8	719.6	EyebrowMedQuart_L
-83.4	38.6	719.7	EyebrowLatQuart_L
-77.1	48.3	718	EyebrowLat_L
-91.9	0	722.2	Head_Glabella
-97	0	654.6	Nose_Subnasale
-89.8	0	702.6	Nose_Sellion
-96.8	0	691.5	Nose_Rhinion
-105.2	0	679.8	Nose_Supratip
-112.2	0	666.5	Nose_Pronasale
-87.3	-11.2	690.2	Nose_Width_R
-87.3	11.2	690.2	Nose_Width_L
-85.2	-21.8	662.8	Nose_AlarCurve_R
-85.2	21.8	662.8	Nose_AlarCurve_L
-91.2	-12.7	656	Nose_Subalare_R
-91.2	12.7	656	Nose_Subalare_L

Table 7C
Head Landmarks Group C (mm)

X	Y	Z	Landmark Name
-82.2	-26.2	627.6	Lips_Chelion_R
-82.2	26.2	627.6	Lips_Chelion_L
-99.6	0	638.4	Lips_LabialeSup
-95	0	629	Lips_Stomion
-97	0	619.5	Lips_LabialeInf
-88.1	0	610.4	Lips_Sublabiale
-81.6	0	584.8	Chin_Gnathion
-89.2	0	597.5	Chin_Pogonion
-35.4	0	568.9	Chin_Cervical
-0.2	-70.6	637.1	Gonion_R
-0.2	70.6	637.1	Gonion_L
19.5	0	817.3	HeadTop
114.1	0	722.2	HeadBack
99.7	0	664.4	Head_Occiput

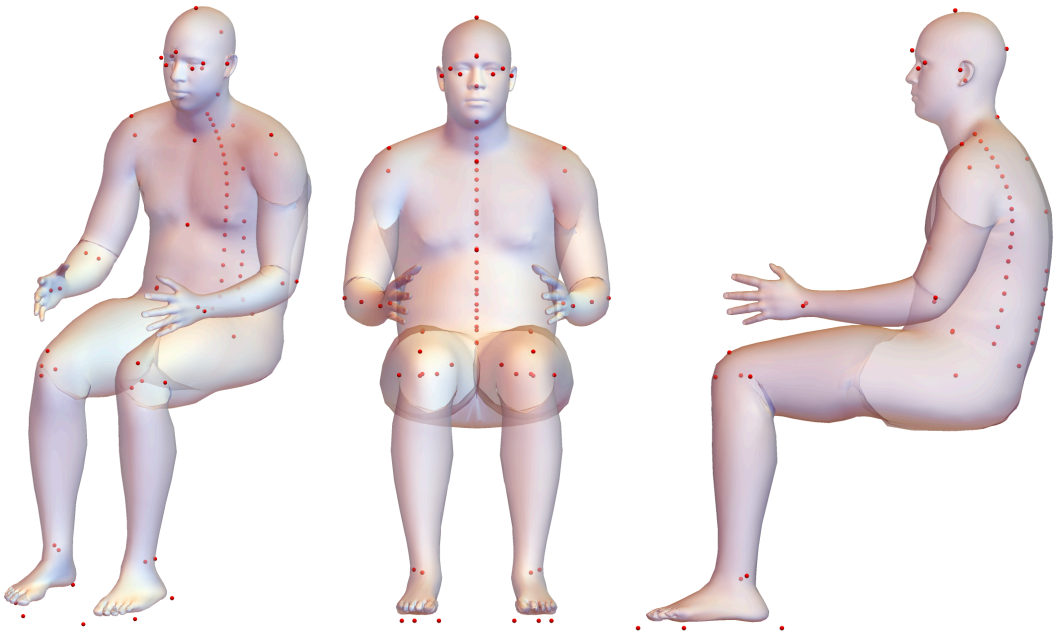

Figure 9. Final body shape after posture adjustment with landmarks, joints, and integrated head, hands, and feet. Note that foot landmarks are on perimeter of boot. See Tables 5A-5C for quantitative information on landmark and joint locations.

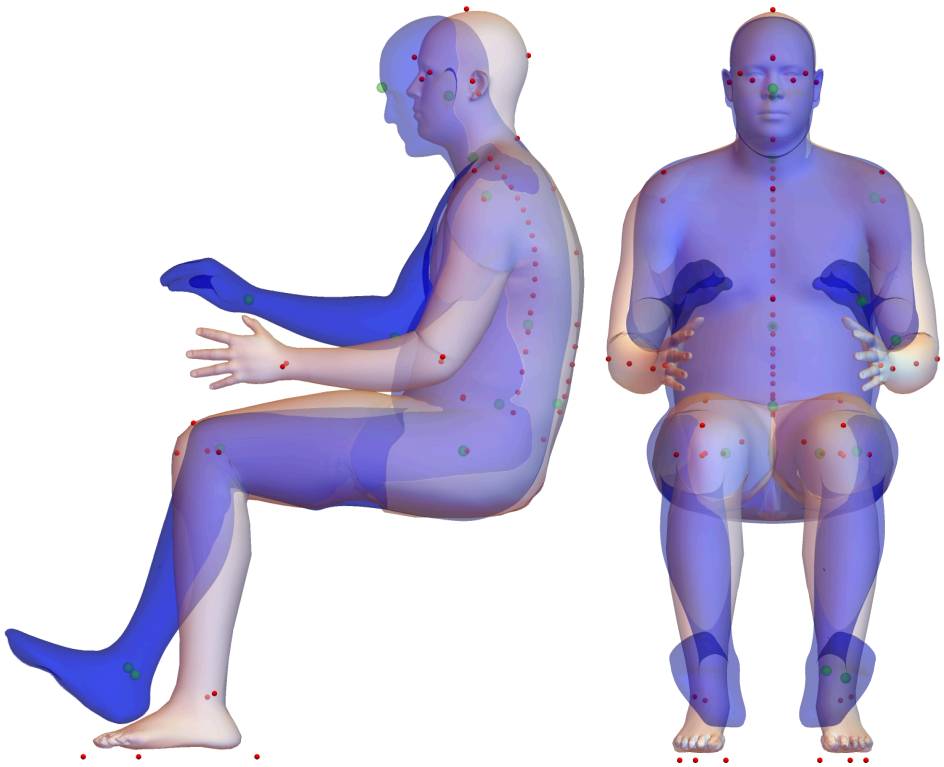

Figure 10. Comparison of the large-male WIAMan external body shape with the large-male AMVO shell (blue). The AMVO shell was aligned to the large-male WIAMan shell at the hip joints and rotated around the Y axis to align at the cervicale (C7 surface) landmark. The AMVO shell represents a typical driving posture with a seat back angle of about 22 degrees.

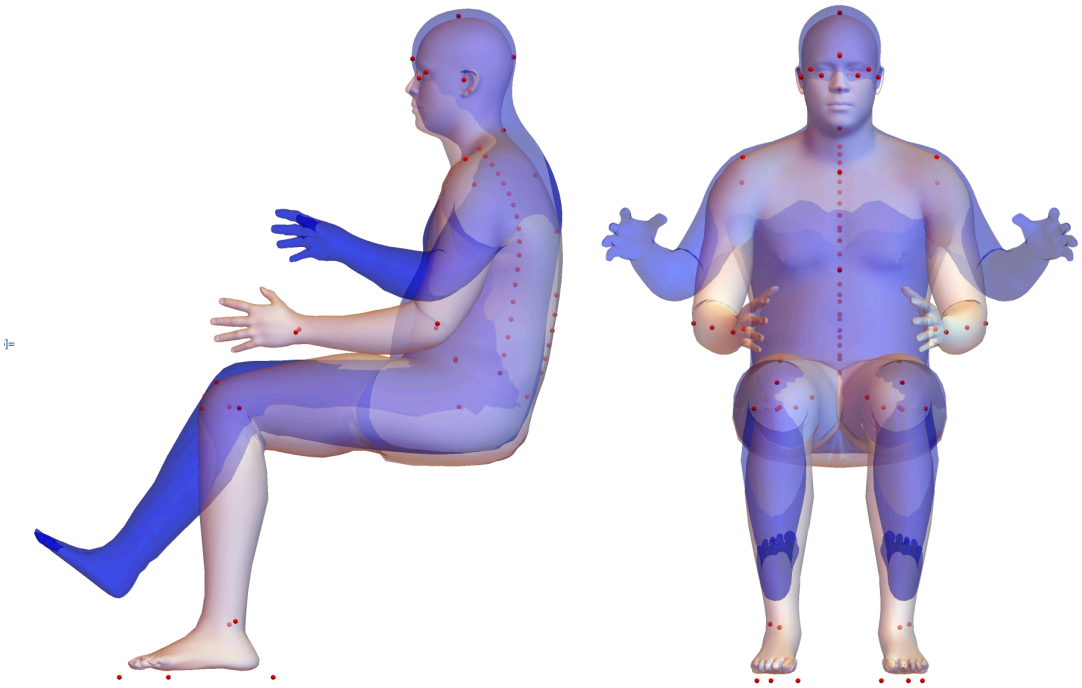

Figure 11. Comparison of the large-male WIAMan external body shape with a BioHuman large-male shell (blue) generated using a statistical body shape model for civilians (Park et al. 2021a, HumanShape.org). The BioHuman shell was aligned to the large-male WIAMan shell at the hip joints and rotated around the Y axis to approximately align the upper thorax. The BioHuman shell represents a typical driving posture.

Pelvis Geometry

Tables 8A and 8B list selected pelvis landmark locations in the WIAMan design position. Figures 11 and 12 illustrate the pelvis alone and in position inside the body surface.

Table 8A
Pelvis Landmarks Group A (mm)

X*	Y	Z	Landmark
16.1	-120.7	91.2	1_ASIS_L
15.8	121.4	91.5	2_ASIS_R
4.1	-101.4	53.1	4_AIIS_L
3.8	100.6	53.3	5_AIIS_L
17.2	-108.9	68.6	6_AS_mid_L
17	108.6	68.6	7_AS_mid_R
143.5	-41.9	13.4	8_PSIS_L
143.9	42.1	13.7	9_PSIS_R
-39.5	-4.2	26.6	16_PS_Sup_L
-39.5	4.2	26.6	20_PS_Sup_R
75.2	-1.1	64.9	24_S1_Ant
110.2	-0.8	65.3	25_S1_Post
93	-28.8	68	26_S1_Left
93.1	27.9	69.2	27_S1_R
61.9	0	-61.9	32_Coccyx
-16.3	-38.9	-69	87_IT_L
-15.8	39.2	-69.5	93_IT_R
0	-90	0	HipJntLt
0	90	0	HipJntRt

* Origin is at midpoint between hip joint centers. X is fore-aft, Y is lateral, Z is vertical.

Table 8B
Pelvis Landmarks Group B (mm)

X*	Y	Z	Landmark
40.6	-135.3	97.1	33_LatIliacCrest1_L
69.3	-143.1	93.7	34_LatIliacCrest2_L
98.1	-136.4	91.2	35_LatIliacCrest3_L
122.1	-117.5	91.5	36_LatIliacCrest4_L
139.5	-93.7	83.5	37_LatIliacCrest5_L
147.9	-69.9	66.3	38_LatIliacCrest6_L
149.7	-55.2	39.7	39_LatIliacCrest7_L
40.2	135.6	97.6	47_LatIliacCrest1_L
69.1	142.9	93.8	48_LatIliacCrest2_R
97.7	136.2	90.8	49_LatIliacCrest3_R
121.7	117.6	91.1	50_LatIliacCrest4_R
139.3	93.8	83.5	51_LatIliacCrest5_R
148	70	66.7	52_LatIliacCrest6_R
149.5	55.7	39.9	53_LatIliacCrest7_R
-0.5	-69.7	-17.5	67_Acet1_L
30.7	-95.7	-13.1	69_Acet2_L
15.4	-104.4	24.9	71_Acet3_L
-12	-72.9	14.6	73_Acet4_L
-0.6	69.2	-16.6	75_Acet1_L
30.4	95.9	-13.4	77_Acet2_L
15.6	104.3	25.6	79_Acet3_L
-12.7	73.1	15.3	81_Acet4_L

* Origin is at midpoint between hip joint centers. X is fore-aft, Y is lateral, Z is vertical.

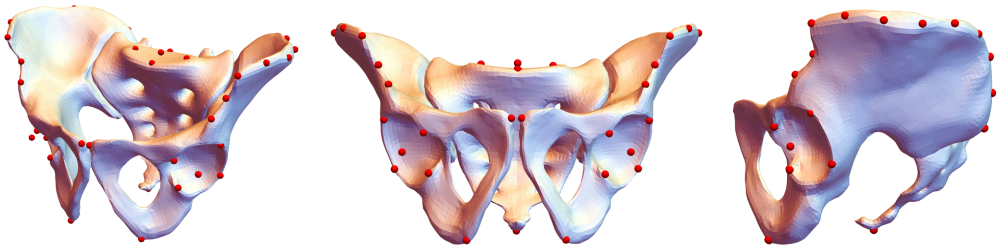

Figure 11. Pelvis geometry and landmarks at design orientation.

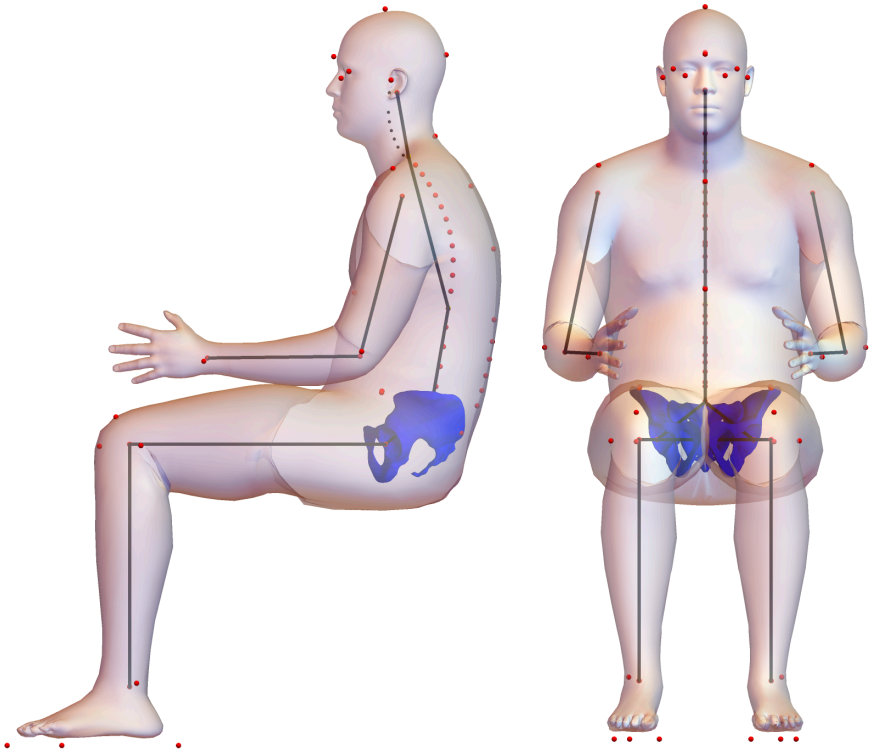

Figure 12. External body shape with pelvis in position. Note foot landmarks are on boot and buttock shape approximates undeformed contour.

DISCUSSION

The anthropometric specifications developed for the large-male WIAMan reflect the best available information on the posture and body shape of seated Soldiers with the reference body dimensions. The surface landmark locations and external body shape are based on a statistical analysis of data measured from Soldiers in a range of postures close to the design posture. The internal joint center location estimates are based on calculation methods developed in prior studies.

This study advanced the methods used to develop the anthropometric specifications for the midsize-male WIAMan in several ways. First, the body shape model is based on a symmetrical polygonal template, unlike the unstructured template used in the prior work. This enabled symmetry to be enforced, providing a better target for design. Second, the head shape is based on a full 3D shape analysis, whereas the prior head was based on a landmark-only analysis that was used to morph a head template. The new head model is also fully integrated into the whole-body template. Third, the pelvis analysis used a new, larger dataset based on a more complete landmarking of pelvis geometry extracted from medical imaging studies.

This work is limited by the size and composition of the dataset used for each of the analysis components. A larger dataset might have yielded slightly different results, and differences in the composition of the sample with respect to race/ethnicity and age would influence the results. However, the posture and body shape outcomes are based on data from a convenience sample of Soldiers that is well matched to US Army personnel (see Reed and Ebert 2013). The body shape modeling method relies on statistical techniques and linear blend skinning to adjust the shape to the target posture. This enables representation of a posture measured in a realistic seat in which the whole-body shape cannot be measured, but the posture adjustments, both through the statistical modeling and linear blend skinning, were not explicitly validated. The hands and feet were not modeled in detail and were instead scaled linearly from the template based on the stature. Additional guidance for the ATD hand and foot designs have been separately provided to the ATD designers.

The internal joint center estimates are based on the same methods used for the midsize male, with some adjustments based on more-recent data from medical imaging studies. The segment length analysis shows reasonable consistency with prior work for the major body segments, but the discrepancies in the lower extremities may reflect difference in populations between the current sample and other representations of large men.

The ATD shape is expected to differ in a variety of ways from these specifications. Notably, the ATD buttock and thigh shape will be adjusted to best reflect the fabrication and performance requirements. Differences are also expected in the joint areas to reflect the range of motion requirements for the ATD. Simplifications of details in the face and other areas are also expected.

REFERENCES

Bennink, H.E., Korbeeck, J.M., Janssen, B.J., and Romenij, B.M. (2006). Warping a neuro-anatomy atlas on 3D MRI data with radial basis functions. *Proceedings of the 2006 International Conference on Biomedical Engineering*. pp. 214-218.

Black, D.M., Cummings, S.R., Stone, K., Hudes, Palermo, L., and Steiger, P. (1991). A new approach to defining normal vertebral dimensions. Journal of Bone and Mineral Research, 6(8):883-892.

Brynskog, E., Iraeus, J., Reed, M.P., and Davidsson, J. (2021). Predicting pelvis geometry using a morphometric model with overall anthropometric variables. *Journal of Biomechanics*, 126. 10.1016/j.jbiomech.2021.110633

Fryar, C.D., Carroll, M.D., Gu, Q/, Afful. J., and Ogden, C.L. (2021). Anthropometric reference data for children and adults: United States, 2015–2018. National Center for Health Statistics. Vital Health Stat 3(46).

Gordon CC, Churchill T, Clauser CE, Bradtmiller B, McConville JT, Tebbetts I, and Walker RA (1989) *1988 Anthropometric Survey of U.S. Army Personnel: Methods and Summary Statistics*. NATICK/TR-89/044. U.S. Army Natick Soldier Research, Development, and Engineering Center, Natick, MA.

Gordon, C. C., Blackwell, C. L., Bradtmiller, B., Parham, J. L., Barrientos, P., Paquette, S. P., and Mucher, M. (2014). 2012 Anthropometric Survey of Marine Corps Personnel: Methods and Summary Statistics. (NATICK/TR-15/007). Army Natick Soldier Research Development and Engineering Center, Natick, MA.

Mertz, H.J, Jarrett, K., Moss, S., Salloum, M., and Zhao, Y. (2001). The Hybrid III 10-year-old dummy. *Stapp Car Crash Journal,* 45:319-328.

Paquette, SP, Gordon CC, and Bradtmiller B (2009) *ANSUR II Pilot Study: Methods and Summary Statistics*. NATICK/TR-09/014. U.S. Army Natick Soldier Research, Development, and Engineering Center, Natick, MA.

Park, B. K. D., Jones, M. L., Ebert, S., and Reed, M. P. (2021a). A Parametric Modeling of Adult Body Shape in a Supported Seated Posture Including Effects of Age. *Ergonomics*. 10.1080/00140139.2021.1992020.

Park, B-K., Corner, B.D., Hudson, J.A., Whitestone, J., Mullenger, C.R., and Reed, M.P. (2021b). A three-dimensional parametric adult head model with representation of scalp shape variability under hair, Applied Ergonomics, 90: 103239

Reed, M.P. (2013). Development of Anthropometric Specifications for the Warrior Injury Assessment Manikin (WIAMan). Technical Report UMTRI-2013-38. University of Michigan Transportation Research Institute, Ann Arbor, MI

Reed, M.P. and Corner, B.D. (2013). Generation of a Midsize-Male Headform by Statistical Analysis of Shape Data. Technical Report UMTRI-2013-39. University of Michigan Transportation Research Institute, Ann Arbor, MI.

Reed, M.P., Ebert, S.M, and Corner, B.D. (2013). Statistical Analysis to Develop a Three-Dimensional Surface Model of a Midsize-Male Foot. Technical Report UMTRI-2013-40. University of Michigan Transportation Research Institute, Ann Arbor, MI.

Reed, M.P. and Ebert, S.M. (2013). The Seated Soldier Study: Posture and Body Shape in Vehicle Seats. Technical Report 2013-13. University of Michigan Transportation Research Institute, Ann Arbor, MI.

Reed, M.P., Manary, M.A., and Schneider, L.W. (1999). Methods for measuring and representing automobile occupant posture. Technical Paper 990959. Society of Automotive Engineers, Warrendale, PA.

Schneider, L.W., Robbins, D.H., Pflüg, M.A., and Snyder, R.G. (1983). Anthropometry of Motor Vehicle Occupants: Development of anthropometrically based design specifications for an advanced adult anthropomorphic dummy family, Volume 1. Final report DOT-HS-806-715. U.S. Department of Transportation, National Highway Traffic Safety Administration, Washington, DC.

Wang, Y., Cao, L., Bai, Z., Reed, M.P., Rupp, J.D., Hoff, C.N., and Hu, J. (2016) A parametric ribcage geometry model accounting for variations among the adult population. *Journal of Biomechanics*, 49(13): 2791-2798